Chapter 3

The Formation of a QGP

3.1 Deconfinement in Heavy Ion Collisions

Under given conditions of temperature and density the hadronic matter undergoes a phase transition towards a plasma of deconfined quarks and gluons. The possibility of obtaining energy densities which are large enough to cause deconfinement in ultra-relativistic heavy ion collisions has acted as one of the main stimuli to interest in such collisions, from both the experimental and theoretical points of view.

Historically, much of the early interest in the deconfinement transition came from the cosmological community, where the emphasis was on hadronization in the early universe. The resulting calculations tended to be performed at zero net baryon number, as befits the early universe scenario. More recently, the high energy physics community, spurred by the development of more powerful particle accelerators, have considered the possibility of obtaining the reverse process, i.e. deconfinement, in the laboratory from ultra-relativistic heavy ion collisions. These collisions result in systems which certainly have non-zero baryon number; as a result, much effort has been devoted to determine full phase diagrams for strongly interacting systems. The major theoretical thrusts in this direction have centered on two approaches, namely lattice QCD and phenomenological models. While lattice QCD [3, 4, 5, 6, 7] is the preferred method of studying the behavior of strongly interacting systems, the enormous computational requirements of such calculations have led to an appreciable amount of work being directed towards phenomenological descriptions of deconfinement [9].

In phenomenological calculations the relevant quantities are the densities of the thermodynamic variables. Anticipating the formation of a QGP during a heavy ion collision, it is at present by no means clear whether there is sufficient time available for the hadron gas and the QGP to equilibrate, and therefore whether traditional equilibrium thermodynamics should be applied to these systems. In what follows, we will assume that the system is in fact in equilibrium. However, the limitations inherent in this assumption should be borne in mind when using the results of our calculations in analysis of heavy ion collisions [9]. We now turn to the description of the system in the QGP phase.

3.2 The QGP Phase

In this approach, the quarks and gluons are treated as forming an ideal gas, apart from the non-perturbative corrections to the pressure and energy density resulting from the bag model [2]. We initially (3.2.1) describe the system by BG statistics in order to define our notations and general numerical procedure. In (3.2.2) we lay out the differences due to the non-extensive statistics. We emphasize that only (3.2.2) can incorporate the anticipated *long-range* forces in the QGP phase.

3.2.1 Boltzmann-Gibbs (BG) Statistics

According to the BG statistics the energy density, pressure, and baryon number density for a QGP consisting of massless up and down quarks and antiquarks, each with degeneracy factor $d_Q = 12$ (2 (spin) x 3 (color) x 2 (quarks and antiquarks)), and gluons, with degeneracy $d_G = 16$ (2 (spin) x 8 (color)), at a temperature T and baryon chemical potential μ are given by (see Appendix C for details)

$$u_{QGP} = \frac{d_Q}{2\pi^2}\int_0^\infty dk\, k^3\,(\bar{n}_Q + \bar{n}_{\bar{Q}}) + \frac{d_G}{2\pi^2}\int_0^\infty dk\, k^3\,\bar{n}_G + B \tag{3.1}$$

$$P_{QGP} = \frac{d_Q T}{2\pi^2}\int_0^\infty dk\, k^2\left\{\ln\left[1+\exp\frac{1}{T}(\mu_Q - k)\right] + \ln\left[1+\exp\frac{-1}{T}(\mu_Q + k)\right]\right\}$$
$$-\frac{d_G T}{2\pi^2}\int_0^\infty dk\, k^2\,\ln\left[1-\exp\left(\frac{-k}{T}\right)\right] - B \tag{3.2}$$

and

$$n_{QGP} = \frac{d_Q}{6\pi^2}\int_0^\infty dk\, k^2\,(\bar{n}_Q - \bar{n}_{\bar{Q}})\,, \tag{3.3}$$

where

$$\bar{n}_{Q(\bar{Q})} = \frac{1}{\exp\frac{1}{T}(k \mp \mu_Q) + 1}\,, \tag{3.4}$$

$$\bar{n}_G = \frac{1}{\exp\left(\frac{k}{T}\right) - 1} \tag{3.5}$$

and $\mu_Q = \frac{\mu}{3}$.

Integration by parts of (3.2) yields

$$P_{QGP} = \frac{1}{3}\,(u_{QGP} - 4B)\,. \tag{3.6}$$

Evaluating the integrals in (3.1-3.3) yields (see Appendix C)

$$u_{QGP} = \frac{\pi^2}{30}\left(d_G + \frac{7}{4}d_Q\right)T^4 + \frac{d_Q\,\mu^2\,T^2}{36} + \frac{d_Q\,\mu^4}{648\,\pi^2} + B\,, \tag{3.7}$$

$$P_{QGP} = \frac{\pi^2}{90}\left(d_G + \frac{7}{4}d_Q\right)T^4 + \frac{d_Q\,\mu^2\,T^2}{108} + \frac{d_Q\,\mu^4}{1944\,\pi^2} - B \tag{3.8}$$

and

$$n_{QGP} = d_Q \left(\frac{\mu\, T^2}{54} + \frac{\mu^3}{486\, \pi^2} \right) , \tag{3.9}$$

where B is the bag constant which is taken here as $(210\ \text{MeV})^4$ [1] with an uncertainty of $\approx 15\%$.

3.2.2 Generalized Statistics

The quantum mechanical distribution function proposed by Buyukklic and Demirhan (BD) [42] is given by

$$\bar{n}_i = \frac{1}{[1 + (q-1)\beta(\epsilon_i - \mu)]^{\frac{1}{q-1}} \mp 1}, \tag{3.10}$$

where the upper and lower signs correspond to bosons and fermions, respectively.

Extremizing the entropic functional,

$$S_q^{(B)} = \sum_i \left[\frac{\bar{n}_i - \bar{n}_i^q}{q-1} - \frac{(1+\bar{n}_i) - (1+\bar{n}_i)^q}{q-1} \right], \tag{3.11}$$

under the constraints imposed by (2.10) and (2.11) yields the q-generalized BD Bose-Einstein distribution, which is given by (3.10) with the minus sign. A "probabilistic" interpretation of the entropic measure (3.11) and the associated variational procedure leading to BD approach distribution for bosons (3.10) is somewhat problematic [39]. If we use the generalized statistics to describe the entropic measure of the whole system, the distribution function can not , in general, be reduced to a finite, closed, analytical expression [39, 43, 44, 45, 46, 47]. For this reason, we use generalized statistics to describe the entropies of the individual particles, rather than of the system as a whole. Even in this case, we are unable to obtain the "probabilistic" interpretation for bosons (see Appendix B).

The single particle distribution functions of quarks, antiquarks and gluons are given by

$$\bar{n}_{Q(\bar{Q})} = \frac{1}{\left[1 + \frac{1}{T}(q-1)(k \mp \mu_Q)\right]^{\frac{1}{q-1}} + 1} \tag{3.12}$$

and

$$\bar{n}_G = \frac{1}{\left[1 + \frac{1}{T}(q-1)k\right]^{\frac{1}{q-1}} - 1}, \tag{3.13}$$

respectively. In the limit $q \to 1$, (3.12) and (3.13) reduce to (3.4) and (3.5) respectively.

The expression for the pressure is given by

$$P_{QGP} = \frac{d_Q\,T}{2\,\pi^2} \int_0^\infty dk\,k^2 \left(\frac{f_Q^{q-1} - 1}{q-1} + \frac{f_{\bar{Q}}^{q-1} - 1}{q-1} \right) - \frac{d_G\,T}{2\,\pi^2} \int_0^\infty dk\,k^2 \left(\frac{f_G^{q-1} - 1}{q-1} \right) - B, \tag{3.14}$$

where

$$f_Q = 1 + \left[1 + \frac{1}{T}(q-1)(k - \mu_Q)\right]^{\frac{1}{1-q}}, \tag{3.15}$$

$$f_{\bar{Q}} = 1 + \left[1 + \frac{1}{T}(q-1)(k + \mu_Q)\right]^{\frac{1}{1-q}} \tag{3.16}$$

and

$$f_G = 1 - \left[1 + \frac{1}{T}(q-1)k\right]^{\frac{1}{1-q}}, \tag{3.17}$$

which in the limit $q \to 1$ reduces to (3.2).

Since the integrals in (3.1-3.3) are not integrable analytically, one has to calculate these integrals numerically. For $q > 1$, the quantity $[1 + \frac{1}{T}(q - 1)(k - \mu_Q)]$ becomes negative if $\mu_Q > k$. To avoid this problem we use [48],

$$f_Q = 1 + \left[1 + \frac{1}{T}(q-1)(k - \mu_Q)\right]^{\frac{1}{1-q}}, \qquad k \geq \mu_Q \tag{3.18}$$

and

$$f_Q = 1 + \left[1 + \frac{1}{T}(1-q)(k - \mu_Q)\right]^{\frac{1}{q-1}}, \qquad k < \mu_Q\,. \tag{3.19}$$

In the limit $q \to 1$ one recovers, of course, the appropriate Fermi-Dirac distribution in both cases. We now turn to the hadronic phase of the system which is more readily accessible to experiment.

3.3 The Hadron Phase

The hadron phase is taken to contain only interacting nucleons and antinucleons and an ideal gas of massless pions motivated by the findings in [49, 50]. The interactions between nucleons can be treated either by means of an excluded volume approximation or by a mean field approximation.

3.3.1 The Excluded Volume Approximation

In this approximation, the short range repulsive hadron-hadron interactions are taken into account by a Van der Waals-type method. The assumption is that a hadron is deformable, but has an intrinsic hard-core volume V_o which prevents compression of the hadron gas beyond a close-packing density $\frac{1}{V_o}$. One of the problems of the excluded volume is this close-packing density; the physics in such a limit is by no means clear. The hard-core volumes of hadrons are taken into account in calculations by reducing the total volume available to the system from V to $V - \sum_i N^i V_o^i$, where N^i is the number of hadrons of species i and V_o^i is the hard-core volume of these species [9].

We consider a nucleon which consists of a meson cloud and a hard-core volume where the quarks reside. The relationship between the hard-core volume V_0 and the hard-core radius R_0 is $V_0 = \frac{4}{3}\pi R_0^3$, where the hard-core radius R_0 is in the range between 0.5 and 1 fm [51, 52]. In the simplest approximation, one can assume that all baryons have the same hard-core volume, and use the relevant value of V_o (e.g. the nucleon volume) for all baryons, and ignore the meson hard-cores altogether. Alternatively, one can assume a parameterization of the hard-core volume in terms of the hadron mass. One such parameterization, which draws its inspiration from the MIT bag model [53], is

$$V_o^i = \frac{m^i}{m_N} V_o^N, \tag{3.20}$$

where m_N is the nucleon mass and V_o^N is the nucleon hard-core volume.

Once the form of the hard-core volume has been determined, the particle number density n^i, the energy density u^i and the pressure P^i are given by [54]

$$n^i = \frac{n_{id}^i}{1 + \sum_j V_o^j n_{id}^j}, \tag{3.21}$$

$$u^i = \frac{u_{id}^i}{1 + \sum_j V_o^j n_{id}^j} \tag{3.22}$$

and

$$P^i = \frac{P_{id}^i}{1 + \sum_j V_o^j n_{id}^j}, \tag{3.23}$$

where the quantities with subscript *id* refer to the relevant quantities calculated for an ideal gas of point-like particles.

While the excluded volume approximation (3.21-3.23) with various volume corrections has been widely used as a method of including hadron-hadron interactions in phenomenological hadron gas models, all such formulations suffer from two main and severe deficiencies [54, 55, 56, 57, 58]. Firstly, the equations of state (EOS) in these models are not *thermodynamically consistent* because we do not have a well defined partition function or thermodynamic potential Ω such that the baryon number N, energy E, pressure P and entropy S can be obtained directly from it (i.e. $N \neq -\left(\frac{\partial\Omega}{\partial\mu}\right)_{T,V}$, $E \neq \left(\frac{\partial}{\partial\beta}\{\beta\Omega\}\right)_{V,\mu} + \mu N$, $P \neq -\left(\frac{\partial\Omega}{\partial V}\right)_{T,\mu}$ and $S \neq -\left(\frac{\partial\Omega}{\partial T}\right)_{V,\mu}$). The second and more crucial deficiency is that these models violate *causality* at high densities, i.e. information travels at a speed larger than the speed of light. Several proposals appeared in the literature which removed the *inconsistency* problem [59, 60, 61, 62, 63, 64] but they suffer from the *causality* problem.

It is possible to construct a *thermodynamically consistent* model using an excluded volume approximation by formulating the problem in the pressure ensemble [59, 60, 61, 62, 63, 64]. For simplicity, let's consider one particle species with eigenvolume v. The pressure P is related to the grand partition function $\mathcal{Z}$ according to

$$P(T,\mu) = T \lim_{V\to\infty} \frac{\ln \mathcal{Z}(T,\mu,V)}{V}\,. \tag{3.24}$$

where μ, T and V are the chemical potential, temperature and volume of the system respectively.

The grand partition function is defined as

$$\mathcal{Z}(T,\mu,V) = \sum_{N=0}^{\infty} \exp\left(\frac{\mu N}{T}\right) Z(T,N,V)\,. \tag{3.25}$$

To introduce the excluded volume, it is necessary to substitute the canonical partition function Z in (3.25) by [63]

$$Z^{excl}(T,N,V) = Z(T,N,V - v\,N)\,\theta(V - v\,N). \tag{3.26}$$

This ansatz is motivated by considering N particles with eigenvolume v in a volume V as N point-like particles in the "available volume", $V - v\,N$. Substituting (3.26) in (3.25), one obtains

$$\mathcal{Z}^{excl}(T,\mu,V) = \sum_{N=0}^{\infty} \exp\left(\frac{\mu N}{T}\right) Z(T,N,V - v\,N)\,\theta(V - v\,N). \tag{3.27}$$

The main problem in evaluating (3.27) is the dependence of the available volume on the varying number of particles N. To overcome this difficulty one has to perform a Laplace transformation of (3.27). This method of the "isobaric partition function" [65] was successfully used [60, 61, 66] to investigate the excluded volume effect in a gas of quark-gluon bags. In doing so, one obtains [63]

$$\hat{\mathcal{Z}}^{excl}(T,\mu,x) \equiv \int_0^\infty dV\,\exp(-x\,V)\,\mathcal{Z}^{excl}(T,\mu,V)$$

$$= \int_0^\infty d\hat{V}\,exp(-x\,\hat{V})\,\mathcal{Z}(T,\hat{\mu},\hat{V})\,, \tag{3.28}$$

where $\hat{\mu} \equiv \mu - v\,T\,x$ and $\hat{V} \equiv V - v\,N$.

From the definition of the pressure function one concludes that the grand canonical partition function of the system, in the thermodynamical limit, approaches

$$\mathcal{Z}^{excl}(T,\mu,V)|_{V\to\infty} \sim \exp\left[\frac{P^{excl}(T,\mu)\,V}{T}\right].$$

From the first equality in (3.28) one sees that this exponentially increasing part of $\mathcal{Z}^{excl}(T,\mu,V)$ generates an extreme right singularity in the function $\hat{\mathcal{Z}}^{excl}(T,\mu,x)$ at some point x^*. For $x < P^{excl}/T$ the integration over V for $\hat{\mathcal{Z}}^{excl}(T,\mu,x)$ diverges at its upper limit. Therefore, the extreme right singularity of $\hat{\mathcal{Z}}^{excl}(T,\mu,x)$ at $x^*(T,\mu)$ gives a pressure [63],

$$P^{excl}(T,\mu) \equiv T \lim_{V\to\infty} \frac{\ln \mathcal{Z}^{excl}(T,\mu,V)}{V} = T\,x^*(T,\mu). \tag{3.29}$$

The direct connection of the extreme right x-singularity of $\hat{\mathcal{Z}}^{excl}$ to the asymptotic behavior $V \to \infty$ of $\mathcal{Z}^{excl}$ is a general mathematical property of the Laplace transform. Using the above equations one obtains

$$x^*(T,\mu) = \lim_{\hat{V}\to\infty} \frac{\ln \mathcal{Z}(T,\tilde{\mu},\hat{V})}{\hat{V}}\ ;\ \tilde{\mu} = \mu - v\,T\,x^*(T,\mu).$$

Applying (3.24) for $\mathcal{Z}(T,\tilde{\mu},\hat{V})$ and making use of (3.29) to eliminate x^* one gets

$$P^{excl}(T,\mu) = P(T,\tilde{\mu})\ ;\ \tilde{\mu} = \mu - v\,P^{excl}(T,\mu). \tag{3.30}$$

Therefore, we have an implicit equation for $P^{excl}(T,\mu)$ if P is a known function of its arguments.

If we consider the ideal gas case, we have in (3.28)

$$\mathcal{Z}_{id}(T,\tilde{\mu},\hat{V}) = \exp[\hat{V}\,F(T,\tilde{\mu})]\,, \tag{3.31}$$

where

$$F(T,\mu) = \frac{1}{a}\frac{d}{(2\pi)^3}\int d^3k\,\ln\left[1 + a\exp\left(\frac{-\sqrt{k^2+m^2}+\mu}{T}\right)\right], \tag{3.32}$$

where $a = \pm 1$ refers for fermions/bosons and $a \to 0$ for classical (Boltzmann) approximation. Performing the integral in (3.28) yields

$$\hat{\mathcal{Z}}^{excl}_{id}(T,\mu,x) = \frac{1}{x - F(T,\hat{\mu})}\,,$$

which gives

$$P^{excl}_{id}(T,\mu) = T\,F(T,\tilde{\mu}) = P_{id}\left(T,\mu - v\,P^{excl}_{id}(T,\mu)\right). \tag{3.33}$$

This is a special case of (3.30) for the ideal gas [62, 67]. The expression (3.30) is valid also for more general cases.

The particle number density, the entropy density and the energy density can be found from (3.33) using the relations [63]

$$n^{excl}_{id}(T,\mu) \equiv \left(\frac{\partial P^{excl}_{id}}{\partial \mu}\right)_T = \frac{n_{id}(T,\tilde{\mu})}{1 + v\,n_{id}(T,\tilde{\mu})}\,, \tag{3.34}$$

$$s^{excl}_{id}(T,\mu) \equiv \left(\frac{\partial P^{excl}_{id}}{\partial T}\right)_\mu = \frac{s_{id}(T,\tilde{\mu})}{1 + v\,n_{id}(T,\tilde{\mu})} \tag{3.35}$$

and

$$u^{excl}_{id}(T,\mu) \equiv T\,s^{excl}_{id} - P^{excl}_{id} + \mu\,n^{excl}_{id} = \frac{u_{id}(T,\tilde{\mu})}{1 + v\,n_{id}(T,\tilde{\mu})}\,, \tag{3.36}$$

where n_{id}, s_{id} and u_{id} are the well-known expressions for an ideal gas of point-like particles. The relations (3.33-3.36) are *thermodynamically consistent*, i.e. fundamental thermodynamical relations are fulfilled.

Since the excluded volume approximation suffers from the *causality* problem even if the *consistency* problem is addressed, we use the relativistic mean field or Hartree approximation proposed by Walecka [68, 69], which is *thermodynamically self-consistent*, to treat the interactions.

3.3.2 The Mean Field Approximation

In this approximation, the interaction between nucleons is described by the *scalar-isoscalar* ϕ and *vector-isoscalar* V^μ mesonic fields with baryon-meson interaction terms in the Lagrangian: $g_s\bar{\psi}\psi\phi$ and $g_v\bar{\psi}\gamma_\mu V^\mu\psi$. For nuclear matter in thermodynamical equilibrium these mesonic fields (ϕ and V^μ) are considered to be *constant* classical quantities. The *scalar* field ϕ describes the attraction between nucleons and lowers the nucleon (antinucleon) mass M to $M^* = M - g_s < \phi >$. The nucleon-nucleon repulsion is described by the *vector* field V^μ which changes the nucleon (antinucleon) energy by $(\pm U(n))$ [1].

The Lagrangian density in the in the Walecka model is given by [70]

$$\mathcal{L} = \bar{\psi}\left[\gamma_\mu\left(i\partial^\mu - g_v V^\mu\right) - (M - g_s\phi)\right]\psi + \frac{1}{2}\left(\partial_\mu\phi\partial^\mu\phi - m_s^2\phi^2\right)$$
$$-\frac{1}{4}F_{\mu\nu}F^{\mu\nu} + \frac{1}{2}m_v^2 V_\mu V^\mu + \delta\mathcal{L}, \tag{3.37}$$

where $F^{\mu\nu} = \partial^\mu V^\nu - \partial^\nu V^\mu$ and $\delta\mathcal{L}$ contains renormalization counterterms required for quantum field theory. The parameters M, g_s, g_v, m_s and m_v are phenomenological constants that can be determined from experimental measurements.

The Euler-Lagrange equations [70]

$$\frac{\partial}{\partial x^\mu}\left[\frac{\partial\mathcal{L}}{\partial(\partial q_i/\partial x^\mu)}\right] - \frac{\partial\mathcal{L}}{\partial q_i} = 0\,, \tag{3.38}$$

[1] The odd G-parity of the ω-meson is responsible for the attractive ω-exchange in $N\bar{N}$ scattering as compared to the repulsive ω-exchange in $NN(\bar{N}\bar{N})$ scattering.

where q_i is one of the generalized coordinates (ψ, ϕ and V^μ), yield the field equations

$$\left(\partial_\mu \partial^\mu + m_s^2\right) \phi = g_s \bar{\psi} \psi \,, \tag{3.39}$$

$$\partial_\mu F^{\mu\nu} + m_v^2 V^\nu = g_v \bar{\psi} \gamma^\nu \psi \tag{3.40}$$

and

$$[\gamma^\mu (i\partial_\mu - g_v V_\mu) - (M - g_s \phi)]\psi = 0 \,. \tag{3.41}$$

Equation (3.39) is simply the Klein-Gordon equation with a scalar source, Equation (3.40) looks like massive quantum electrodynamics (QED) with the conserved baryon current

$$B^\mu = \bar{\psi} \gamma^\mu \psi \,; \quad \partial_\mu B^\mu = 0 \tag{3.42}$$

rather than the (conserved) electromagnetic current as source and equation (3.41) is the Dirac equation with the *scalar* and *vector* fields introduced in a minimal fashion. These field equations also imply that the canonical energy-momentum tensor

$$T^{\mu\nu} = i\bar{\psi}\gamma^\mu \partial^\nu \psi - \frac{1}{2}\left(\partial_\sigma \phi \partial^\sigma \phi - m_s^2 \phi^2\right) g^{\mu\nu} + \partial^\mu \phi \partial^\nu \phi$$
$$+\frac{1}{2}\left(\partial_\sigma V_\lambda \partial^\sigma V^\lambda - m_v^2 V_\sigma V^\sigma\right) g^{\mu\nu} - \partial^\mu V_\lambda \partial^\nu V^\lambda \tag{3.43}$$

is conserved ($\partial_\mu T^{\mu\nu} = \partial_\nu T^{\mu\nu} = 0$).

Equations (3.39-3.41) are *nonlinear quantum field equations*, and their exact solutions are very complicated. In particular, they describe mesons and baryons that are not *point like particles*, but rather objects with intrinsic structure due to the implied (virtual) mesonic and baryon-antibaryon loops. When the source terms are large, the meson field operators can be replaced by their expectation values, which are classical fields [70]:

$$\phi \rightarrow <\phi> \equiv \phi_0 \,; \quad V^\mu \rightarrow <V^\mu> \equiv \delta^{\mu 0} V_0 \tag{3.44}$$

For a static, uniform system, the quantities ϕ_0 and V_0 are *constants* that are independent of space and time. Rotational invariance implies that the expectation value of the three-vector piece of V^μ vanishes.

The meson field equations (3.39) and (3.40) can be solved for constants ϕ_0 and V_0 to give

$$\phi_0 = \frac{g_s}{m_s^2} < \bar{\psi}\psi > \tag{3.45}$$

and

$$V_0 = \frac{g_v}{m_v^2} < \psi^\dagger\psi > . \tag{3.46}$$

When the meson fields in (3.41) are approximated by the classical fields of (3.44), the Dirac equation becomes *linear*,

$$[i\gamma_\mu\partial^\mu - g_v\gamma^0 V_0 - (M - g_s\phi_0)]\psi = 0 \tag{3.47}$$

and can be solved exactly. It is this *linearization* of the full field equation (3.41) that allows the baryons to be interpreted as *point particles.* As for free particles, the stationary state solutions for a uniform system have the form

$$\psi = \psi(\mathbf{k}, \lambda)e^{i\mathbf{k}\cdot\mathbf{x} - i\epsilon(k)t} \tag{3.48}$$

where $\psi(\mathbf{k}, \lambda)$ is a four-component Dirac spinor and λ denotes the spin index, which corresponds to one of the two orthogonal polarizations chosen in the particle's rest frame [70]. The Dirac equation then becomes

$$(\boldsymbol{\alpha}\cdot\mathbf{k} + \beta M^*)\psi(\mathbf{k}, \lambda) = [\epsilon(k) - g_v V_0]\,\psi(\mathbf{k}, \lambda)\,, \tag{3.49}$$

where $\boldsymbol{\alpha}$ and β are the four matrices:

$$\boldsymbol{\alpha} = \begin{pmatrix} 0 & \boldsymbol{\sigma} \\ \boldsymbol{\sigma} & 0 \end{pmatrix}, \quad \beta = \begin{pmatrix} 1 & 0 \\ 0 & -1 \end{pmatrix}. \tag{3.50}$$

The *effective* mass M^* is defined by

$$M^* = M - g_s\phi_0\,. \tag{3.51}$$

The condensed *scalar* field ϕ_0 thus serves to shift the mass of the baryons. Evidently, the condensed *vector* field V_0 shifts the frequency (or energy) of the solutions. The square of equation (3.49) and the properties of the Dirac matrices yield the eigenvalue equations [70]

$$\epsilon^{(\pm)}(k) = g_v V_0 \pm \sqrt{k^2 + M^{*2}} \equiv g_v V_0 \pm E^*(k)\,. \tag{3.52}$$

The presence of both positive and negative square roots is the characteristic of the Dirac equation. These solutions can be used to define quantum field operators and the Hamiltonian density for the system can be constructed in the canonical fashion (for the details of these procedures, see ref. [70]). The result is

$$\hat{H} = \hat{H}_{MFT} + \delta H\,, \tag{3.53}$$

$$\hat{H}_{MFT} = g_v V_0 \hat{B} + \sum_{\mathbf{k}\lambda} E^*(k)\left(A^\dagger_{\mathbf{k}\lambda}A_{\mathbf{k}\lambda} + B^\dagger_{\mathbf{k}\lambda}B_{\mathbf{k}\lambda}\right) + \frac{1}{2}V\left(m_s^2\phi^2 - m_v^2 V_0^2\right), \tag{3.54}$$

$$\hat{B} = \sum_{\mathbf{k}\lambda}\left(A^\dagger_{\mathbf{k}\lambda}A_{\mathbf{k}\lambda} - B^\dagger_{\mathbf{k}\lambda}B_{\mathbf{k}\lambda}\right) \tag{3.55}$$

and

$$\delta H = -\sum_{\mathbf{k}\lambda}\left(\sqrt{k^2 + M^{*2}} - \sqrt{k^2 + M^2}\right). \tag{3.56}$$

Here $A^\dagger_{\mathbf{k}\lambda}$, $B^\dagger_{\mathbf{k}\lambda}$, $A_{\mathbf{k}\lambda}$ and $B_{\mathbf{k}\lambda}$ are creation and destruction operators for baryons and antibaryons with shifted mass and energy. The properties of these operators are completely determined by the anticommutation relations:

$$\left\{A_{\mathbf{k}\lambda}, A^\dagger_{\mathbf{k}'\lambda'}\right\} = \delta_{\mathbf{k}\mathbf{k}'}\delta_{\lambda\lambda'} = \left\{B_{\mathbf{k}\lambda}, B^\dagger_{\mathbf{k}'\lambda'}\right\}$$

$$\left\{A_{\mathbf{k}\lambda}, B_{\mathbf{k}'\lambda'}\right\} = 0 = \left\{A^\dagger_{\mathbf{k}\lambda}, B^\dagger_{\mathbf{k}'\lambda'}\right\}, \ etc. \tag{3.57}$$

$\hat{B}$ is the baryon number operator, which clearly counts the number of baryons minus the number of antibaryons, the index λ denotes both spin and isospin projections and the correction term δH arises from placing the operators in $\hat{H}_{MFT}$ in normal order [70].

The thermodynamic potential $\Omega(\mu, V, T)$ can be computed using the standard expression from statistical mechanics:

$$\Omega(\mu, V, T) = -T \ln \left\{ Tr \left[\exp\left(-\frac{\hat{H} - \mu \hat{B}}{T} \right) \right] \right\}, \tag{3.58}$$

where $\hat{H}$ is the Hamiltonian of the mean field theory and μ is the chemical potential of baryons.

The general form of the *thermodynamically self-consistent* EOS for nuclear matter which includes the mean field theory and pure phenomenological models as special cases is [71, 72]:

$$P(T,\mu) = \frac{\gamma_N}{3} \int \frac{d^3k}{(2\pi)^3} \frac{k^2}{\sqrt{k^2 + M^{*2}}} \left(\bar{n}_N + \bar{n}_{\bar{N}}\right) + n\,U(n) - \int_0^n dn'\,U(n') + p(M^*), \tag{3.59}$$

$$\bar{n}_{N(\bar{N})} = \left[\exp\left(\frac{\sqrt{k^2 + M^{*2}} \mp \mu \pm U(n)}{T} \right) + 1 \right]^{-1}, \tag{3.60}$$

$$\left(\frac{\delta p}{\delta M^*} \right)_{T,\mu} \equiv \frac{dp(M^*)}{dM^*} - \gamma_N \int \frac{d^3k}{(2\pi)^3} \frac{M^*}{\sqrt{k^2 + M^{*2}}} \left(\bar{n}_N + \bar{n}_{\bar{N}}\right) = 0, \tag{3.61}$$

$$n(T,\mu) = \gamma_N \int \frac{d^3k}{(2\pi)^3} \left(\bar{n}_N - \bar{n}_{\bar{N}}\right) \tag{3.62}$$

and

$$u(T,\mu) = \gamma_N \int \frac{d^3k}{(2\pi)^3} \sqrt{k^2 + M^{*2}} \left(\bar{n}_N + \bar{n}_{\bar{N}}\right) + \int_0^n dn'\,U(n') - p(M^*), \tag{3.63}$$

where P, n and u are the pressure, baryon number density and energy density respectively, $\bar{n}_{N(\bar{N})}$ is the distribution function of nucleons (antinucleons), μ is the baryon chemical potential and γ_N is the spin-isospin degeneracy of the nucleon which is 4 for symmetric nuclear matter. Equation (3.61) describes the dependence of the effective nuclear mass M^* on T and μ which is defined by extremizing the thermodynamical potential (maximizing the pressure).

If we choose [68, 69],

$$p(M^*) = -\frac{1}{2\,C_s^2}(M - M^*)^2, \qquad U(n) = C_v^2\,n \tag{3.64}$$

where $C_s \equiv g_s\left(\frac{M}{m_s}\right)$ and $C_v \equiv g_v\left(\frac{M}{m_v}\right)$. The parameters M, M^*, g_s, g_v, m_s and m_v are taken here to be M= 0.940 GeV, M^*= 0.543M, $g_s \approx 11$ GeV^{-1}, $g_v \approx 14$ GeV^{-1}, m_s= 0.520 GeV and m_v= 0.783 GeV, which reproduce data (see ref. [70, 72] for details) in the hadronic phase.

The energy density, pressure and baryon number density for the hadron gas taken to contain nucleons, antinucleons and an ideal gas of massless pions are:

$$u_H(T,\mu) = \frac{\gamma_N}{2\,\pi^2}\int_0^\infty dk\,k^2\sqrt{k^2+M^{*2}}\,(\bar{n}_N + \bar{n}_{\bar{N}}) + \frac{1}{2}C_v^2\,n^2 + \frac{1}{2\,C_s^2}(M-M^*)^2 + \frac{1}{10}\pi^2\,T^4\,, \tag{3.65}$$

$$P_H(T,\mu) = \frac{\gamma_N}{6\,\pi^2}\int_0^\infty \frac{dk\,k^4}{\sqrt{k^2+M^{*2}}}\,(\bar{n}_N + \bar{n}_{\bar{N}}) + \frac{1}{2}C_v^2\,n^2 - \frac{1}{2\,C_s^2}(M - M^*)^2 + \frac{1}{30}\pi^2\,T^4 \tag{3.66}$$

and

$$n_H(T,\mu) = \frac{\gamma_N}{2\,\pi^2}\int_0^\infty dk\,k^2\,(\bar{n}_N - \bar{n}_{\bar{N}})\,, \tag{3.67}$$

where $\bar{n}_{N(\bar{N})}$ as in (3.60) with $U(n)$ as in (3.64).

Finally, we address the phase transition from the hadronic to the QGP phase, within our model.

3.4 Phase Transition

Assuming a first order phase transition between hadronic matter and QGP, one matches an EOS for the hadronic system and the QGP via Gibbs conditions for phase equilibrium:

$$P_H = P_{QGP}, \qquad T_H = T_{QGP}, \qquad \mu_H = \mu_{QGP} \tag{3.68}$$

With these conditions the pertinent regions of temperature T and baryon chemical potential μ are shown in figures (3.1-3.3) for $q=$ 1, 1.1 (0.9) and 1.25 (0.75). At low values of μ and T the nuclear matter is composed of confined hadrons, but as the energy density is raised, with increasing T or μ, or both, the hadronic matter undergoes a phase transition towards a plasma of deconfined quarks and gluons. The critical temperature at $\mu = 0$ for $q=$ 1, 1.1 (0.9) and 1.25 (0.75) are found to be 122 MeV, 101 MeV and 66 MeV with B=(180 MeV)^4; 148 MeV, 122 MeV and 79 MeV with B=(210 MeV)^4 and 180 MeV, 148 MeV and 96 MeV with B=(250 MeV)^4, respectively. As the non-extensive parameter deviates from $q=$ 1 to 1.25 (0.75), the critical temperature becomes almost independent of the baryon chemical potential which is associated with the number of particles. Variation of the bag constant B between (180 MeV)^4 and (250 MeV)^4 (fig. 3.1-3.3) and excluding interactions among the constituents in the hadron phase (fig. 3.4) do not alter our findings significantly. One still observes a flattening of the $T(\mu)$ curves as $|1-q|$ increases. The only effect is a shift of the value of the maximal μ and $T(0)$. The agreement between BG and the generalized statistics as the critical temperature approaches to zero is evident from equations (3.2) and (3.14). Figures (3.5-3.7) show the dependence of the critical temperature on the non-extensive parameter at $\mu = 0$, 250 MeV and 1000 MeV. The dependence is almost linear for small values of $|1-q|$

with a slope $|\frac{\Delta T}{\Delta q}| \approx 190$ MeV , $|\frac{\Delta T}{\Delta q}| \approx 240$ MeV, and $|\frac{\Delta T}{\Delta q}| \approx 302$ MeV for B=(180 MeV)^4, B=(210 MeV)^4 and B=(250 MeV)^4, respectively . This can be interpreted as a new type of universality condition [33] which suggests that the formation of a QGP occurs (almost) independent of the total number of baryons participating in heavy ion collisions.

We also consider the extensive Kaniadakis statistics [37, 38] to represent the constituents of the QGP [73]. Figure (3.8) shows the $T(\mu)$ curves for κ=0, κ=0.23 and κ=0.29. Since the two statistics are fractal in nature, we observe a similar flattening of the $T(\mu)$ curves as the deformation κ increases. For κ=0.23 (see fig. 3.9), we obtain essentially the same phase diagram as in the case of Tsallis statistics with q=1.1.

3.5 Conclusion

We have studied the phase transition from a system in the hadronic phase to the QGP phase. The phase diagrams shown in figures (3.1-3.3, 3.8) are for interacting hadrons and non-interacting QGP. Excluding interactions among the constituents in the hadron phase (fig. 3.4) does not change the flattening of the $T(\mu)$ curves. The empirical insensitivity of the phase diagram to *details* of the interactions in the hadron phase shows that the *short-range* interactions among the constituents in the hadron phase are unimportant for the phase transition. On the QGP side the *short-range* interactions have died out (due to "asymptotic freedom") and have made room for the only remaining *long-range* interactions among the constituents. Although we do not explicitly consider the interactions, we account for the dominant part of this interaction by a change in the statistics of the system in the QGP phase.

In the present work, we consider two entropic measures (Tsallis and Kaniadakis) to represent the constituents of the QGP. Both are fractal in nature but differ in that: Tsallis statistics is non-extensive and reduces to BG statistics (extensive) as the Tsallis parameter q tends to one. On the other hand, Kaniadakis statistics is extensive and tends to BG statistics as the deformation parameter κ tends to zero. Due to lack of experimental data, we choose different values of q and κ to determine the phase diagram in both cases. For κ=0.23 (see fig. 3.9), we obtain essentially the same phase diagram as in the case of Tsallis statistics with q=1.1. This agreement suggests that the flattening in the phase diagram is due to the fractal nature of both Tsallis and Kaniadakis statistics.

We present here testable consequences of using extensive and non-extensive form of generalized statistical mechanics on the formation a QGP. The resulting insensitivity of the critical temperature to the total number of baryons presents a clear experimental signature for the existence of generalized statistics for the constituents of the QGP.

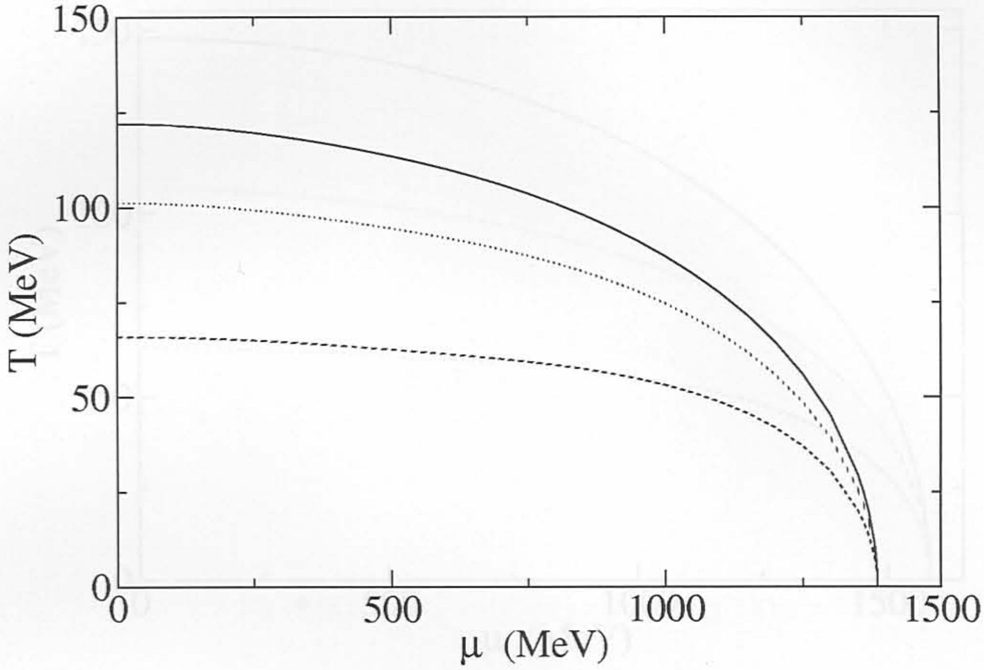

Figure 3.1: Phase transition curves between the hadronic matter and QGP for q=1 (solid line), q=1.1 (0.9) (dotted line) and q=1.25 (0.75) (dashed line) with B=(180 MeV)^4.

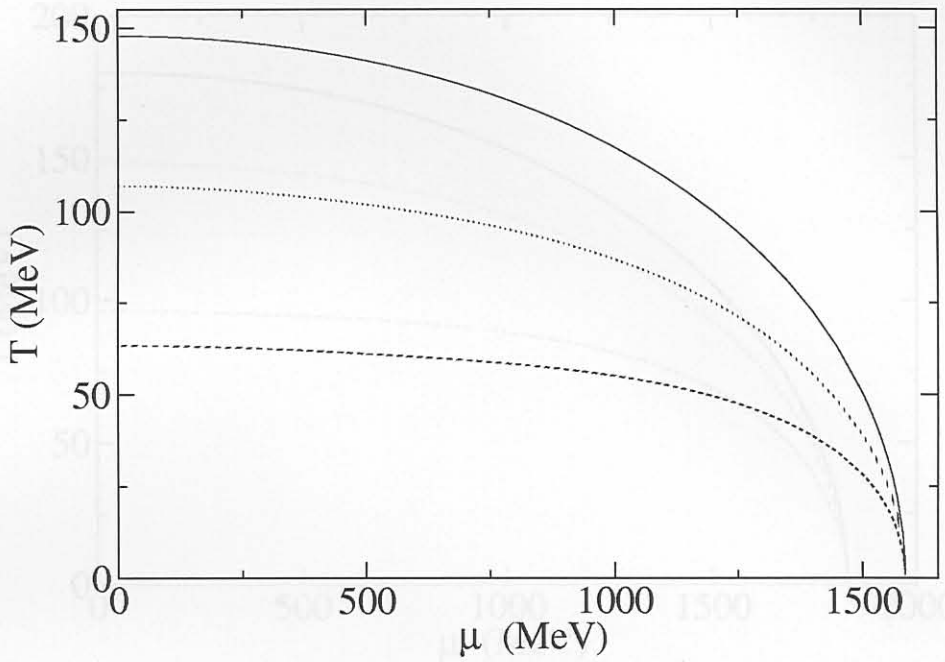

Figure 3.2: Phase transition curves between the hadronic matter and QGP for q=1 (solid line) [1], q=1.1 (0.9) (dotted line) and q=1.25 (0.75) (dashed line) with B=(210 MeV)^4.

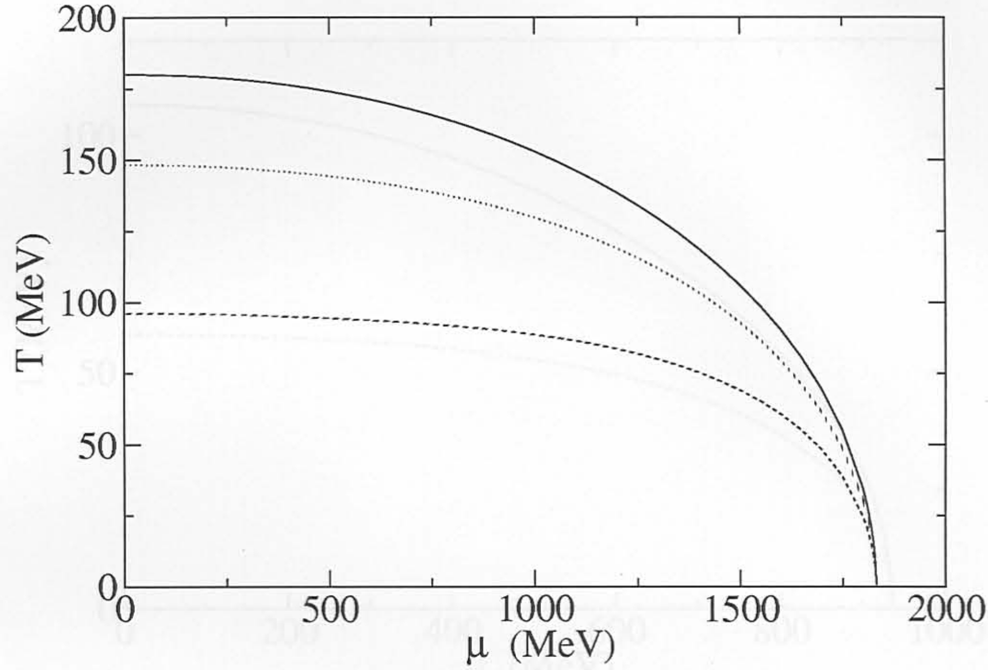

Figure 3.3: Phase transition curves between the hadronic matter and QGP for q=1 (solid line), q=1.1 (0.9) (dotted line) and q=1.25 (0.75) (dashed line) with B=(250 MeV)^4.

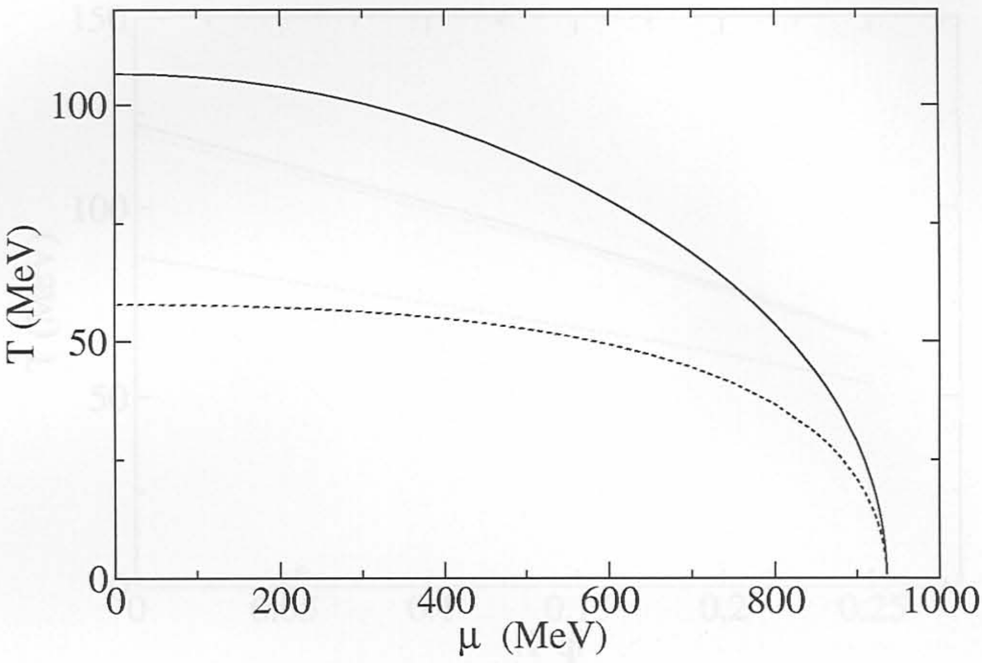

Figure 3.4: Phase transition curves between the hadronic matter and QGP for q=1 (solid line) [2] and q=1.25 (0.75) (dashed line) with B=(148 MeV)^4.

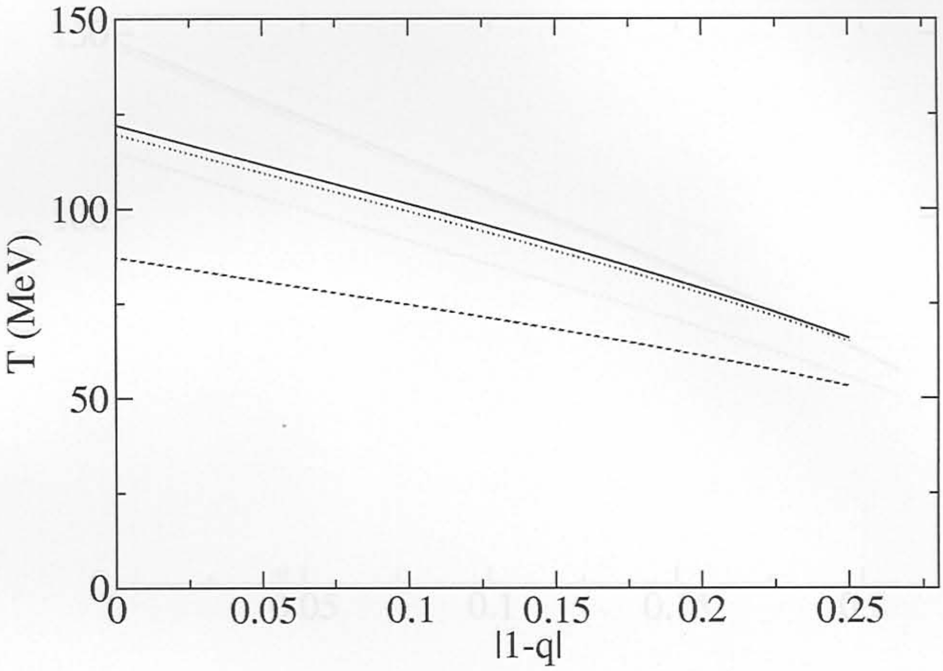

Figure 3.5: The dependence of T on $|1-q|$ at μ= 0 (solid line), μ= 250 MeV (dotted line) and μ= 1000 MeV (dashed line) with B=(180 MeV)^4.

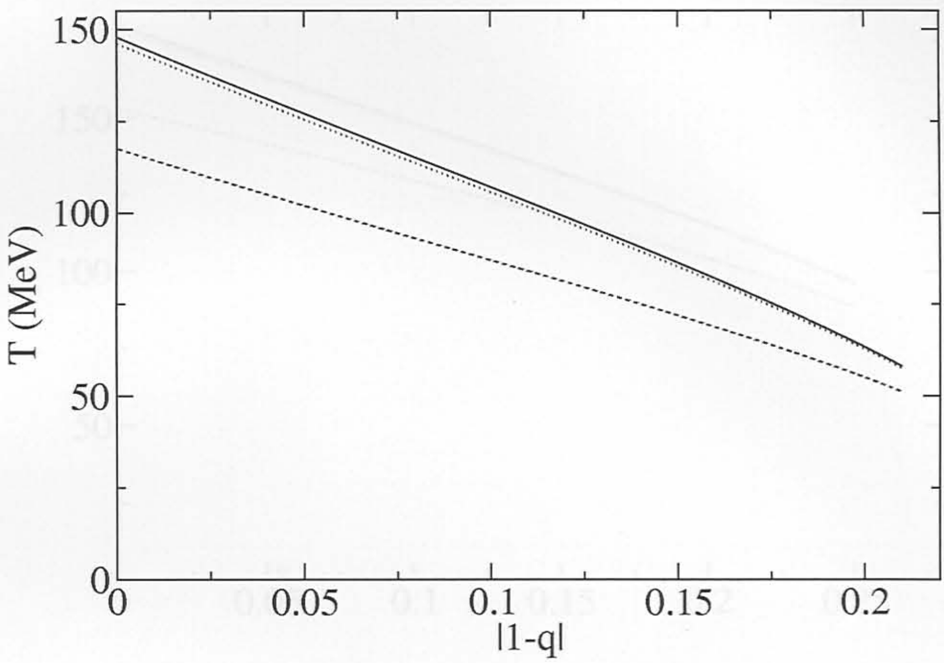

Figure 3.6: The dependence of T on $|1-q|$ at μ= 0 (solid line), μ= 250 MeV (dotted line) and μ= 1000 MeV (dashed line) with B=(210 MeV)^4.

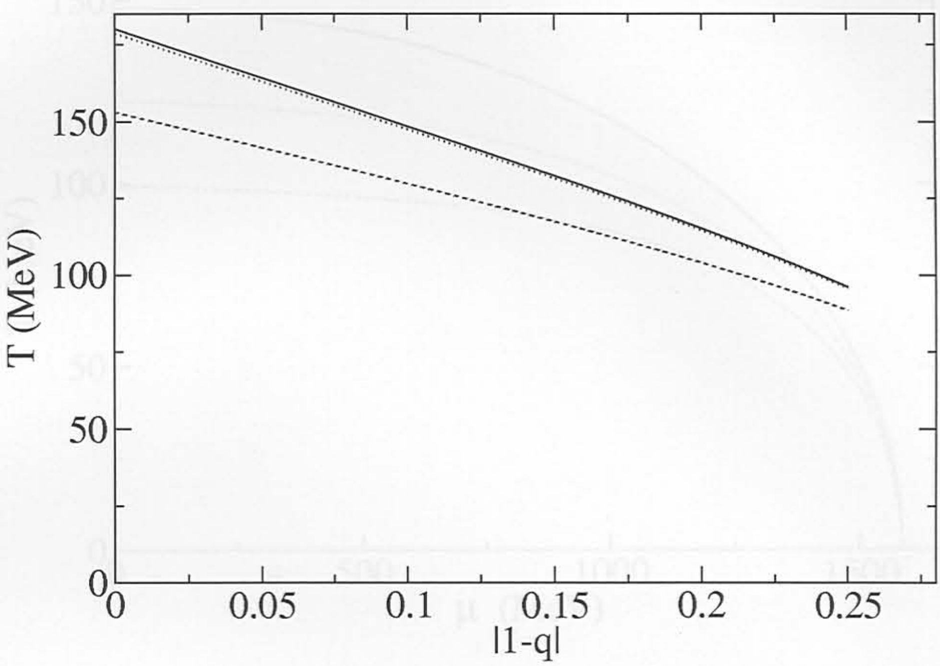

Figure 3.7: The dependence of T on $|1-q|$ at μ= 0 (solid line), μ= 250 MeV (dotted line) and μ= 1000 MeV (dashed line) with B=(250 MeV)^4.

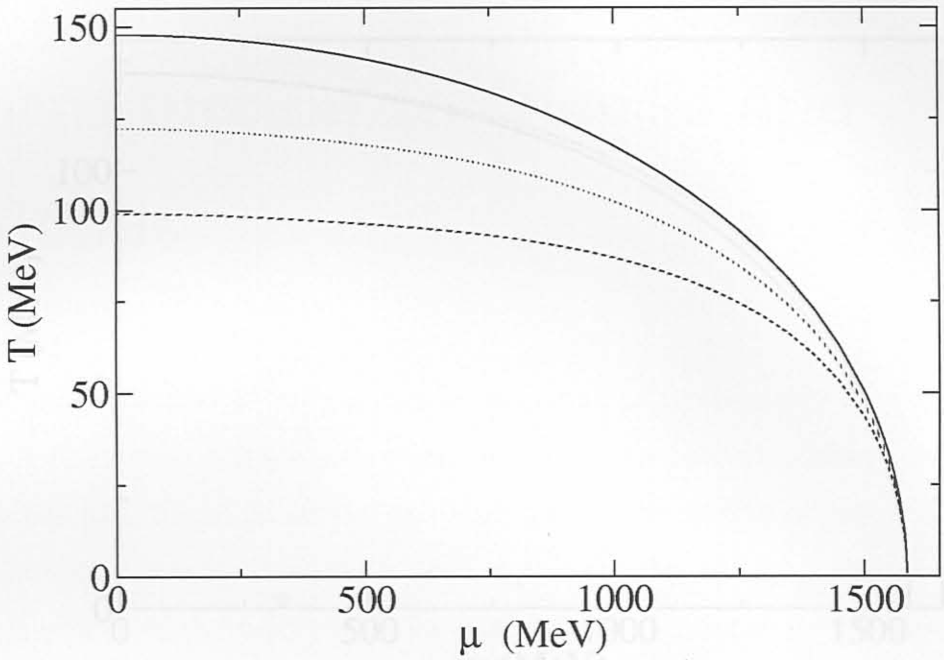

Figure 3.8: Phase transition curves between the hadronic matter and QGP for κ=0 (solid line) [1], κ=0.23 (dotted line) and κ=0.29 (dashed line) with B=(210 MeV)^4.

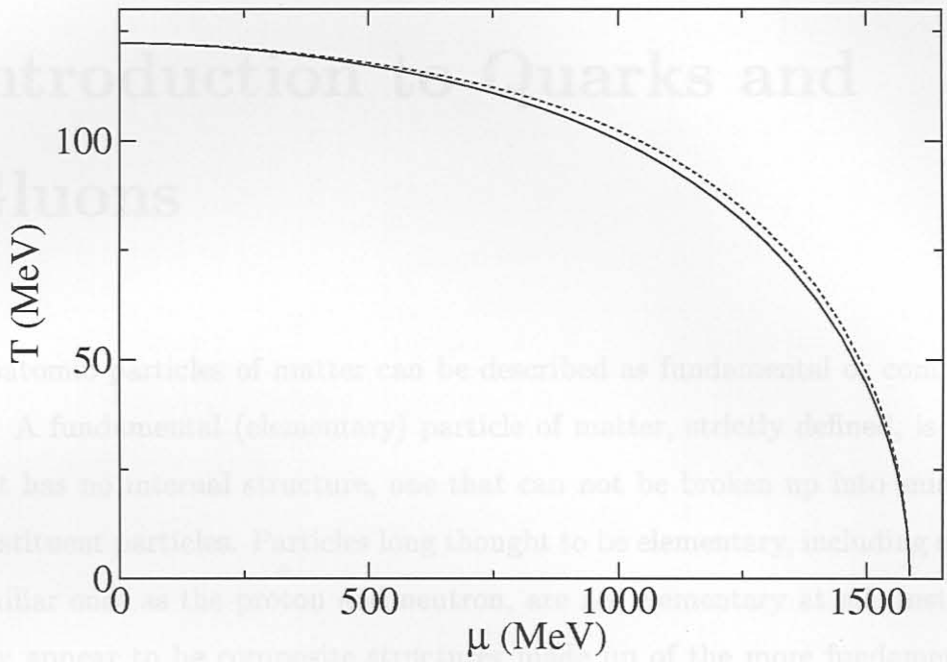

Figure 3.9: Phase transition curves between the hadronic matter and QGP for κ=0.23 (dashed line) and q=1.1 (solid line) with B=(210 MeV)^4.